ISSN 1070-3284, Russian Journal of Coordination Chemistry, 2020, Vol. 46, No. 4, pp. 260–267. © Pleiades Publishing, Ltd., 2020.
Russian Text © The Author(s), 2020, published in Koordinatsionnaya Khimiya, 2020, Vol. 46, No. 4, pp. 241–248.

Molecular Structure and Photoluminescence Behavior of the Zn(II) Carboxylate Complex with Pyrazino[2,3-f][1,10]phenanthroline

S. A. Nikolaevskii[a], D. S. Yambulatov[a, *], A. A. Starikova[b], A. A. Sidorov[a], M. A. Kiskin[a], and I. L. Eremenko[a]

[a] *Kurnakov Institute of General and Inorganic Chemistry, Russian Academy of Sciences, Moscow, 119991 Russia*
[b] *Institute of Physical and Organic Chemistry, Southern Federal University, Rostov-on-Don, 344090 Russia*
**e-mail: yambulatov@igic.ras.ru*

Received October 11, 2019; revised November 25, 2019; accepted November 26, 2019

Abstract—A new complex [Zn(Piv)$_2$(Pyzphen)] (**I**) was prepared by the reaction of pyrazino[2,3-f][1,10]phenanthroline (Pyzphen) with Zn(II) pivalate [Zn(Piv)$_2$]$_n$. An X-ray diffraction study (CIF file CCDC no. 1912821) revealed that complex **I** has a mononuclear structure, with ZnN$_2$O$_4$ coordination unit being a distorted trigonal prism. Quantum chemical simulation of dimerization of complex **I**, resulting in the hypothetical binuclear product [Zn(Piv)$_2$(Pyzphen)]$_2$ (**II**), showed that two energy demanding transition states present on the path of association of the complex molecules may prevent the experimental isolation of binuclear complex **II**. According to the results of luminescence studies of the Pyzphen ligand and complex **I**, the ligand emission band shifts to the blue region upon coordination to zinc(II) ion.

Keywords: zinc(II) complex, structure, photoluminescence, DFT

DOI: 10.1134/S1070328420040053

INTRODUCTION

Zinc carboxylate complexes with N-donor ligands are known to be promising objects for applications in various fields of chemistry, physics, biology, medicine, and many other fields of science and technology as active sites, which often determine the properties of compounds and processes using them. Numerous carboxylate derivatives with zinc(II) ions exhibit biological activities [1, 2], serve as active substances of drugs [3] or precursors of complex oxide materials with unique physical characteristics [4], and are convenient precursors for the chemical assembly of photoluminescent Zn-Ln heterometallic complexes, potential components of photoactive materials [5–8] and porous metal-organic frameworks [9–12]. Note that molecular complexes can themselves exhibit unusual photoactivity [13], in particular, intense ligand-centered luminescence, which largely depends on the nature of substituent in the carboxylate group and the electronic structure of the additional N-donor ligand [14–16], the presence of solvated molecules in the solid phase [17, 18], and packing of molecules in the crystal. As regards the last-mentioned case, the molecules of complexes in the crystalline state can be either packed separately or interact through various intermolecular contacts [19] (H-bonds, stacking, halogen—halogen bonds, and other [20–29]), which opens up the opportunity to control the photophysical characteristics of the crystal. Analysis of the published data reveals increasing interest in the catalytic properties of carboxylate complexes containing zinc ions [30, 31]. For example, the catalytic activity of zinc carboxylates in various processes involving CO$_2$ has been discussed in the literature [32–36].

In view of the foregoing, gaining information about the structure of zinc carboxylate complexes functionalized by additional N-donor ligands, the role of structural effects, and ligand coordination details (steric factors, intra- and intermolecular interactions) is a relevant task. The search for the ways of varying luminescence behavior of these compounds (for example, blue and red shifts upon ligand coordination) can be quite useful for developing processes for targeted synthesis of photoactive d-4f heterometallic complexes containing d^{10} blocks sensitizing the luminescence of lanthanide ions [37–40]. Furthermore, studies of complexes of this type are important for modeling and studying the nature of structure-forming factors responsible for the efficiency of intermolecular interactions, which is necessary for the development of fundamental principles of the chemical design of dynamic molecular crystals with definite adjustable photoluminescence [7, 8, 41], electrophysical [42, 43], catalytic [31], and other practically useful properties [44].

Recently, we studied in detail a wide systematic series of Zn(II) and Cd(II) pivalate complexes functionalized with bi- and tridentate N-donor chelating ligands [45]. In continuation of this study, we prepared a new mononuclear complex $[Zn(Piv)_2(Pyzphen)] \cdot 2C_7H_8$ (Pyzphen is pyrazino[2,3-f][1,10]phenanthroline), determined its molecular and crystal structure, studied the luminescence behavior, and evaluated the possibility of its aggregation in the solid phase (e.g., during crystallization from a solution), in particular, dimerization to give the hypothetical complex $[Zn_2(Piv)_4(Pyzphen)_2]$.

EXPERIMENTAL

All synthetic operations were carried out in air using commercially available solvents: acetonitrile (Khimmed, reagent grade), toluene (Khimmed, reagent grade), and Pyzphen (Sigma-Aldrich, 99%). The complex $[Zn(Piv)_2]_n$ was synthesized by a known procedure [46].

Attenuated total reflectance (ATR) IR spectrum of the compound was measured in the 400–4000 cm^{-1} range on a Perkin Elmer Spectrum 65 spectrophotometer equipped with a Quest ATR Accessory attachment (Specac). Elemental analysis was performed on a EuroEA-3000 automatic C,H,N,S-analyzer (EuroVektor). The excitation and emission spectra of solid samples were measured at room temperature in the visible spectral range on a Perkin-Elmer LS-55 spectrometer.

Synthesis of $[Zn(Piv)_2(Pyzphen)] \cdot 2C_7H_8$ (I · $2C_7H_8$). Pyrazino[2,3-f][1,10]phenanthroline (0.0232 g, 0.1 mmol) was added to a suspension of $[Zn(Piv)_2]_n$ (0.0268 g, 0.1 mmol) in acetonitrile (10 mL). The obtained mixture was vigorously stirred at 60°C for 2 h. After cooling to room temperature, the resulting transparent solution was kept in an open beaker for 48 h. The glassy mass formed upon evaporation of most of acetonitrile was recrystallized from acetonitrile (5 mL), and then toluene (5 mL) was added. The solution thus formed was kept in an open 25-mL conical flask for 24 h, which resulted in the formation of large single crystals of complex **I** · $2C_7H_8$. The yield was 0.0451 g (66%).

For $C_{38}H_{42}N_4O_4Zn$

Anal. calcd., %	C, 66.71	H, 6.18	N, 8.19
Found, %	C, 66.60	H, 6.00	N, 8.30

ATR IR (ν, cm^{-1}): 2958 m, 2869 w, 1591 s, 1558 s, 1495 m, 1481 vs, 1404 vs, 1390 s, 1360 s, 1311 m, 1216 s, 1172 m, 1125 w, 1083 s, 1030 m, 1003 w, 966 w, 893 s, 839 s, 824 vs, 809 s, 793 s, 732 vs, 711 m, 696 vs, 647 m, 667 w, 613 s, 538 w, 466 s, 435 s, 418 vs.

Single crystal X-ray diffraction study of complex **I** · $2C_7H_8$ was performed on a Bruker APEX II diffractometer (CCD detector, MoK_α, $\lambda = 0.71073$ Å, graphite monochromator) [47]. Semiempirical absorption corrections were applied [48]. The structure was solved by the direct and Fourier methods and refined in the full-matrix anisotropic approximation for all non-hydrogen atoms. The hydrogen atoms attached to carbon atoms of organic ligands were generated geometrically and refined in the riding model. The calculations were done using the SHELXL-2014/6 program package [49]. Crystallographic parameters and structure refinement details for complex **I** · $2C_7H_8$: $C_{38}H_{42}N_4O_4Zn$, $M = 684.12$, crystal size: 0.40 × 0.30 × 0.25 mm, colorless parallelepipeds, $T = 296(2)$ K, monoclinic system with space group $P2/c$, $a = 12.1112(13)$, $b = 11.9092(12)$, $c = 14.0018(15)$ Å, $\beta = 112.184(2)°$, $V = 1870.1(3)$ Å^3, $Z = 2$, $\rho = 1.215$ g/cm^3, $\mu = 0.699$ mm^{-1}, $\theta = 2.32°–26.37°$, $-15 \le h \le 15$, $-14 \le k \le 14$, $-17 \le l \le 17$; 13579 measured reflections, 3819 unique reflections, 2804 reflections with $I \ge 2\sigma(I)$, $R_{int} = 0.0371$, $T_{min}/T_{max} = 0.740/0.832$, GOOF = 1.442, $R_1 = 0.0805$, $wR_2 = 0.1622$ (for all data), $R_1 = 0.0581$, $wR_2 = 0.1524$ (for $I \ge 2\sigma(I)$), $\Delta\rho_{min}/\Delta\rho_{max} = -0.489/0.366$ e Å^{-3}.

Additional crystallographic parameters for structure **I** · $2C_7H_8$. were deposited with the Cambridge Crystallographic Data Centre (CCDC no. 1912821; deposit@ccdc.cam.ac.uk or http://www.ccdc.cam.ac.uk).

Quantum chemical calculations were performed using the Gaussian 09 program [50] by density functional theory (DFT) with the B3LYP functional [51], which adequately reproduces characteristics of metal coordination compounds [45, 52–55], and the Def2SVP basis set. The stationary points on the potential energy surface (PES) were identified by full optimization of the geometry of the molecular structures with DFT wavefunction stability check. The dimerization mechanism of the complex was studied by searching for all stationary points along the reaction path. The transition states were located using the standard procedure of the Gaussian software (Opt = TS, calcfc). The fact that the identified transition states belong to the discussed mechanism was ascertained by gradient descent in the positive and negative directions of the gradient vector, which had an imaginary eigenvalue (imaginary frequency). The graphical images of molecular structures were obtained using the ChemCraft program [56], in which the Cartesian coordinates of atoms found by quantum chemical calculations were used as the input parameters.

RESULTS AND DISCUSSION

The reaction of the zinc(II) coordination polymer $[Zn(Piv)_2]_n$ with a stoichiometric amount (1 : 1) of bidentate chelating N-donor ligand, pyrazino[2,3-f][1,10]phenanthroline, gave the coordination compound $[Zn(Piv)_2(Pyzphen)]$. The complex was isolated from an acetonitrile–toluene mixture (1 : 1) as single crystals suitable for X-ray diffraction.

Table 1. Selected bond lengths, bond angles, and intermolecular contacts for $[Zn(Piv)_2(Pyzphen)] \cdot 2C_7H_8$*

Bond	*d*, Å	Angle	ω, deg
Zn(1)–N(1)	2.118(2)	O(1)Zn(1)O(1*A*)	139.72(17)
Zn(1)–O(1)	2.012(2)	O(1)Zn(1)N(1*A*)	111.95(10)
Zn(1)–O(2)	2.377(3)	O(1)Zn(1)N(1)	99.27(11)
O(1)–C(1)	1.250(4)	O(1*A*)Zn(1)N(1*A*)	99.27(11)
O(2)–C(1)	1.226(5)	O(1*A*)Zn(1)N(1)	111.95(10)
N(1)–C(10)	1.326(4)	N(1)Zn(1)N(1*A*)	78.07(12)
N(1)–C(6)	1.353(3)	O(1)Zn(1)O(2*A*)	99.22(11)
N(2)–C(12)	1.324(5)	O(1)Zn(1)O(2)	58.27(11)
N(2)–C(11)	1.357(4)	N(1)Zn(1)O(2)	147.65(11)
C(6)–C(6*A*)$^{\#1}$	1.461(5)	N(1)Zn(1)O(2*A*)	88.88(9)
C(11)–C(11*A*)	1.403(6)	O(1*A*)Zn(1)O(2*A*)	58.27(11)
C(12)–C(12*A*)	1.365(8)	O(1*A*)Zn(1)O(2)	99.22(11)
		N(1*A*)Zn(1)O(2)	88.88(9)
		N(1*A*)Zn(1)O(2*A*)	147.65(11)
		O(2)Zn(1)O(2*A*)	115.83(14)
C–H···O	C···O, Å	H···O, Å	CHO angle, deg
C(9)–H(9)···O(1*D*)$^{\#2}$	3.339(4)	2.54	144.1
C(12)–H(12)···O(2H)$^{\#3}$	3.440(4)	2.60	150.2

* Symmetry codes: $^{\#1}$ $1 - x; y, 1/2 - z$; $^{\#2}$ $1 - x, 1 - y, -z$; $^{\#3}$ $1 - x, -1 + y, 1/2 + z$.

According to X-ray diffraction data, the compound crystallizes in monoclinic space group $P2/c$ as a solvate with two toluene molecules. A twofold axis passes through the Zn(1) atom and between the carbon atoms of the C(6)–C(6*A*), C(11)–C(11*A*), and C(12)–C(12*A*) bonds of the coordinated Pyzphen molecule (Fig. 1a). Selected bond lengths and bond angles of complex **I** · $2C_7H_8$ are summarized in Table 1. The ZnN_2O_4 coordination polyhedron, formed by two N atoms of the chelating Pyzphen molecule and four O atoms of the chelating carboxylate groups, is a distorted trigonal prism (D_{3h}, $S_Q(P)$ = 6.174) according to calculations using the SHAPE 2.1 software [57]. There are π-stacking interactions between the Pyzphen aromatic moiety C(6)C(7)C(11)C(11*A*)-C(7*A*)C(6*A*) and toluene solvate molecules (the distance between the ring centroids is 3.66 Å; the shortest C(6)···C(1S) distance is 3.434(7) Å; the angle between the ring planes is 12.4(6)°) (Fig. 1a). The intermolecular C–H···O bonds between the H atoms of Pyzphen and O atoms of the carboxylate groups of the adjacent molecules of the complex (each molecule of the complex forms eight C–H···O bonds with four adjacent molecules) give rise to a supramolecular network in the *bc* plane (Fig. 1b, Table 1).

Unlike zinc pivalate adducts with 2,2'-bipyridine, 1,10-phenanthroline and its substituted analogues, and with 2,2':6',2''-terpyridine [45], which we described previously, the molecules of $[Zn(Piv)_2(Pyzphen)]$ in the crystal are isolated. The formation of π-stacking interactions between the coordinated Pyzphen molecules, giving rise to a supramolecular stack structure, was observed previously for the heterometallic molecular complex $[Zn_2Tb(OH)(Piv)_4(NO_3)_2(Pyzphen)_2] \cdot MeCN$ [58]. Apparently, the π-stacking interactions between the Pyzphen ligands of the neighboring $[Zn(Piv)_2(Pyzphen)]$ molecules is prevented by the interaction with toluene solvate molecules.

Previously, it was shown that cadmium ions form binuclear complexes with 2,2'-bipyridine and bathophenanthroline, while zinc ions form mononuclear compounds under similar conditions, which correlates with the results of quantum mechanical calculations [45]. According to DFT calculations, the formation of binuclear cadmium complexes is barrierless and is accompanied by release of 14.1 kcal/mol of energy. The likely appearance of a possible intermediate and, as a consequence, a transition state on the path of association of zinc complexes indicates that dimerization of zinc(II)-containing monomers should be accompanied by energy expenditure, which accounts for the absence of stable binuclear complexes in the case of zinc derivatives in the series of compounds we studied [45]. To continue these studies, we carried out analogous quantum chemical calculations for $[Zn(Piv)_2(Pyzphen)]$ and its hypothetical dimer

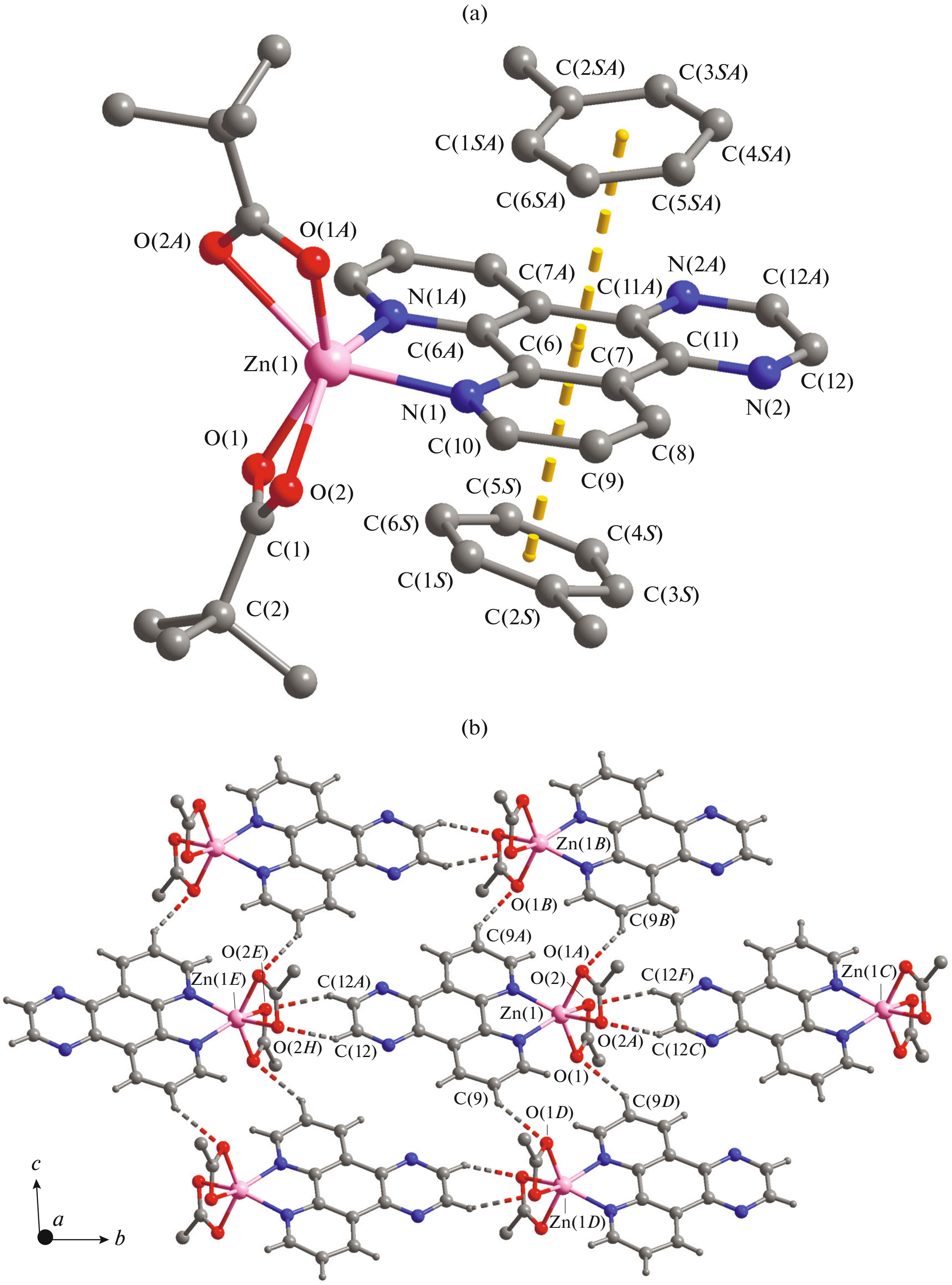

Fig. 1. (a) Molecular structure of the complex [Zn(Piv)$_2$(Pyzphen)] · 2C$_7$H$_8$ (hydrogen atoms are omitted, dashed lines show the interactions between the centroids of aromatic rings); (b) fragment of crystal packing (methyl groups and solvate molecules are not shown). *A*: 1 – *x*, *y*, 1/2 – *z*; *B*: *x*, 1 – *y*, 1/2 + *z*; *C*: *x*, 1 + *y*, *z*; *D*: 1 – *x*, 1 – *y*, –*z*; *E*: *x*, –1 + *y*, *z*; *F*: 1 – *x*, 1 + *y*, 1/2 – *z*; *H*: 1 – *x*, –1 + *y*, 1/2 + *z*.

Table 2. Total energy (E) without and with inclusion of zero-point energy (E^{ZPE}), relative energy (ΔE) without and with inclusion of zero-point energy (ΔE^{ZPE}) calculated by DFT B3LYP/Def2SVP

Structure	E, a.u.	ΔE, kcal/mol	E^{ZPE}, a.u.	ΔE^{ZPE}, kcal/mol
$[Zn(Piv)_2(Pyzphen)]$	−3228.455033		−3227.986915	
$2[Zn(Piv)_2(Pyzphen)]$	−6456.910066	15.6	−6456.973829	15.9
$[Zn(Piv)_2(Pyzphen)]_2$	−6456.934938	0.0	−6455.999169	0.0
A	−6456.921600	8.4	−6455.985522	8.6
B	−6456.928902	3.8	−6455.992884	3.9
TS1	−6456.916950	11.3	−6455.980872	11.5
TS2	−6456.921344	8.5	−6455.985365	8.7

$[Zn(Piv)_2(Pyzphen)]_2$, a formal analogue of the known complex $[Zn(OAc)_2(Phen)]_2$ (Phen = 1,10-phenanthroline) [59].

According to the calculations (Table 2), the stabilization energy of the dimer $[Zn(Piv)_2(Pyzphen)]_2$ with respect to dissociation into two monomers is 15.9 kcal/mol. This value is comparable with that calculated for close analogues with a cadmium(II) ion (14.1 kcal/mol) and formally implies thermodynamic stability of the dimer. However, this result is in sharp contrast with structural characteristics of the zinc(II)-containing molecule. Presumably, the inability of the zinc complex $[Zn(Piv)_2(Pyzphen)]$ to form a dimer is attributable to the mechanism of its formation and crystallization.

In order to confirm this hypothesis, we used the approach comprising examination of the potential energy surface in the dimer dissociation region. For this purpose, the PES of $[Zn(Piv)_2(Pyzphen)]_2$ was scanned by increasing the M–M distance with 0.1 Å increments and with optimization of the other parameters of the reaction system. As shown by calculations (Table 2, Fig. 2), the increase in the Zn···Zn distance is accompanied by cleavage of one pivalate bridge to give an intermediate (A), destabilized relative to the dimer $[Zn(Piv)_2(Pyzphen)]_2$ by 8.6 kcal/mol. The presence of this intermediate in the reaction path indicates that dimerization proceeds via a transition state, which implies existence of an energy barrier. Further increase in the Zn···Zn distance affords a weakly bound dimer (B), which dissociates to give two mononuclear complexes $[Zn(Piv)_2(Pyzphen)]$.

In order to study the dimerization mechanism of the $[Zn(Piv)_2(Pyzphen)]$ monomer, the search for transition states was performed between the minima found during PES scanning. According to calculations, two $[Zn(Piv)_2(Pyzphen)]$ molecules form, without a barrier, weakly bound complex B. As the monomers further approach each other, intermediate A is formed. This process involves transition state (TS1) and proceeds via a barrier of 7.6 kcal/mol. The second transition state (TS2) has geometric and energy parameters close to those of intermediate A (Table 2). The gradient descent from structure TS2 along a gradient vector brings the system to the dimer $[Zn(Piv)_2(Pyzphen)]_2$. The presence of two transition states along the reaction path is probably responsible for the fact that zinc-containing dimer cannot be detected experimentally. The schematic image of the energy profile of $[Zn(Piv)_2(Pyzphen)]$ dimerization is shown in Fig. 3. The results of quantum-chemical calculations allowed to explain stabilization of $[Zn(Piv)_2(Pyzphen)]$ as the monomer.

We investigated the photoluminescence behavior of Pyzphen and its complex. The excitation spectrum of the Pyzphen ligand at λ_{emis} = 550 nm shows bands at 286, 360, and 399 nm (with a shoulder at 425 nm) (Fig. 4). The emission spectrum at λ_{excit} = 400 nm exhibits a broad band with a maximum at 550 nm. The excitation spectrum of the complex $[Zn(Piv)_2(Pyzphen)] \cdot 2C_7H_8$ at λ_{emis} = 538 nm contains a set of bands at 236, 254, 335, 395, and 428 nm (Fig. 4). The emission spectrum of the complex at λ_{excit} = 395 nm consists of a broad band at 538 nm with a shoulder at ~600 nm. The complex formation of Pyzphen with zinc(II) induces a blue shift of the principal emission band of the ligand by 12 nm.

Thus, we synthesized and structurally characterized a new zinc(II) pivalate complex functionalized with a chelating N-donor ligand, pyrazino[2,3-f][1,10]phenanthroline. According to X-ray diffraction data, the complex is mononuclear, the ZnN_2O_4 coordination unit is a distorted trigonal prism. Quantum chemical simulation of dimerization of $[Zn(Piv)_2(Pyzphen)]$, resulting in a hypothetical binuclear product $[Zn(Piv)_2(Pyzphen)]_2$, demon-

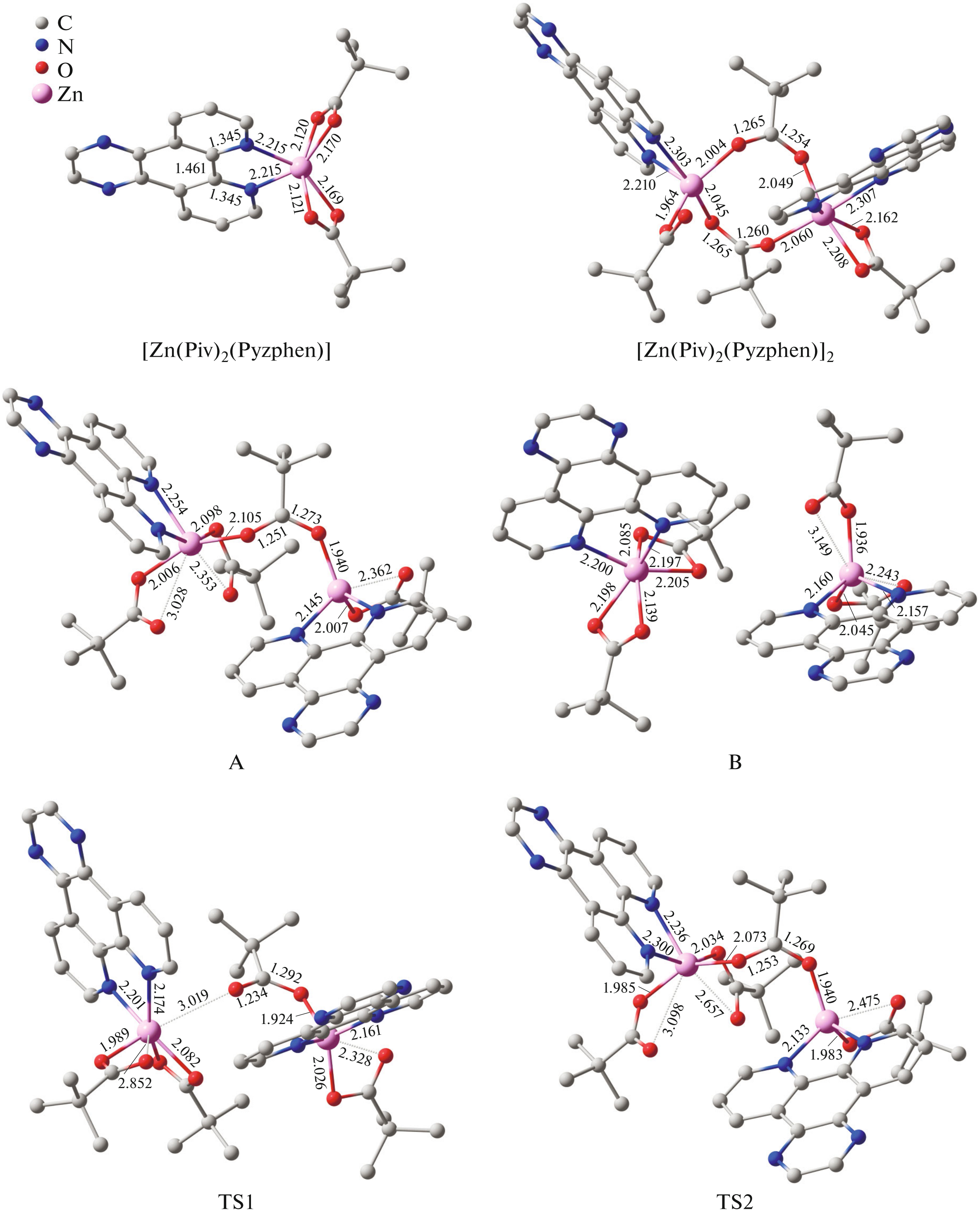

$[Zn(Piv)_2(Pyzphen)]$ $[Zn(Piv)_2(Pyzphen)]_2$

A B

TS1 TS2

Fig. 2. Geometry optimization for the structures obtained by PES scanning, according to DFT B3LYP/Def2SVP calculation results. Hydrogen atoms are omitted, the bond lengths are given in Å.

strated that the presence of two energy-demanding transition states on the path of association of complex molecules may be the factor preventing isolation of the dimer $[Zn(Piv)_2(Pyzphen)]_2$. The obtained calculation results are in full agreement with the data published previously [45]. The results of studies of the photoluminescence behavior of Pyzphen and $[Zn(Piv)_2(Pyzphen)] \cdot 2C_7H_8$ indicated that chelation to the zinc(II) ion induces a blue shift of the principal emission band of the ligand.

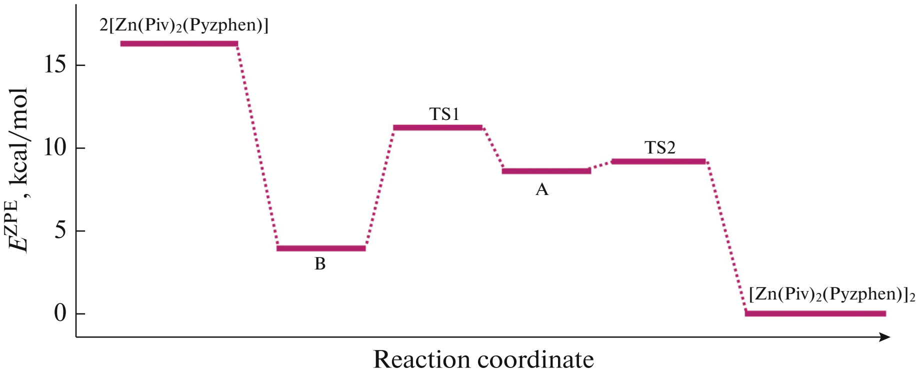

Fig. 3. Schematic view of the mechanism of dimerization of two complexes [Zn(Piv)$_2$(Pyzphen)], according to DFT B3LYP/Def2SVP calculation results.

ACKNOWLEDGMENTS

X-ray diffraction analysis, IR spectroscopy, luminescence, and elemental analysis were performed using equipment of the Center for Collective Use of Physical Investigation Methods, Kurnakov Institute of General and Inorganic Chemistry, Russian Academy of Sciences, within the state assignment of the Kurnakov Institute of General and Inorganic Chemistry, Russian Academy of Sciences, in the field of fundamental research.

FUNDING

This study was supported by the Russian Science Foundation (project no. 16-13-10537).

CONFLICT OF INTEREST

The authors declare that they have no conflicts of interest.

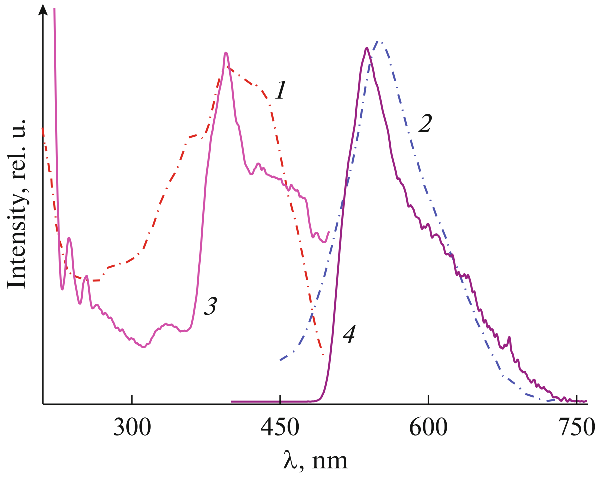

Fig. 4. Excitation and emission spectra of Pyzphen: (*1*) λ_{em} = 550 nm, (*2*) λ_{excit} = 400 nm; [Zn(Piv)$_2$(Pyzphen)] · 2C_7H_8: (*3*) λ_{em} = 538 nm, (*4*) λ_{excit} = 395 nm for solid samples at room temperature.

REFERENCES

1. Abu Ali, H., Fares, H., Darawsheh, M., et al., *Eur. J. Med. Chem.*, 2015, vol. 89, p. 67.
2. Zelenak, V., Györyová, K., and Mlynarcík, D., *Met. Based. Drugs*, 2002, vol. 8, p. 269.
3. Abu Ali, H., Omar, S.N., Darawsheh, M.D., and Fares, H., *J. Coord. Chem.*, 2016, vol. 69, p. 1110.
4. Johnson, A.L., Kingsley, A.J., Kociok-Köhn, G., et al., *Inorg. Chem.*, 2013, vol. 52, p. 5515.
5. Egorov, E.N., Mikhalyova, E.A., Kiskin, M.A., et al., *Russ. Chem. Bull.*, 2013, vol. 62, p. 2141.
6. Sidorov, A.A., Kiskin, M.A., Aleksandrov, G.G., et al., *Russ. J. Coord. Chem.*, 2016, vol. 42, p. 621. https://doi.org/10.1134/S1070328416100031
7. Goldberg, A., Kiskin, M., Shalygina, O., et al., *Chem. Asian J.*, 2016, vol. 11, p. 604.
8. Kiraev, S.R., Nikolaevskii, S.A., Kiskin, M.A., et al., *Inorg. Chim. Acta*, 2018, vol. 477, p. 15.
9. Ding, B., Hua, C., Kepert, C.J., and D’Alessandro, D.M., *Chem. Sci.*, 2019, vol. 10, p. 1392.
10. Fernández-Palacio, F., Restrepo, J., Gálvez, S., et al., *CrystEngComm*, 2014, vol. 16, p. 3376.
11. Sapianik, A.A., Zorina-Tikhonova, E.N., Kiskin, M.A., et al., *Inorg. Chem.*, 2017, vol. 56, p. 1599.
12. Sapianik, A.A., Kiskin, M.A., Kovalenko, K.A., et al., *Dalton. Trans.*, 2019, vol. 48, p. 3676.
13. Fanna, D.J., Zhang, Y., Li, L., et al., *Inorg. Chem. Front.*, 2016, vol. 3, p. 286.
14. Larionov, S.V., Kokina, T.E., Plyusnin, V.F., et al., *Polyhedron*, 2014, vol. 77, p. 75.
15. Mautner, F.A., Berger, C., Fischer, R.C., and Massoud, S.S., *Polyhedron*, 2016, vol. 111, p. 86.
16. Sayapin, Y.A., Nikolaevskii, S.A., Makarova, N.I., et al., *Russ. J. Org. Chem.*, 2016, vol. 52, p. 1018.
17. Adonin, S.A., Sokolov, M.N., Rakhmanova, M.E., et al., *Inorg. Chem. Commun.*, 2015, vol. 54, p. 89.
18. Adonin, S.A., Rakhmanova, M.E., Smolentsev, A.I., et al., *New J. Chem.*, 2015, vol. 39, p. 5529.
19. Varughese, S., *J. Mater. Chem. C*, 2014, vol. 2, p. 3499.
20. Chernyshev, A.N., Morozov, D., Mutanen, J., et al., *J. Mater. Chem.*, C, 2014, vol. 2, p. 8285.

21. Sivchik, V.V., Solomatina, A.I., Chen, Y.-T., et al., *Angew. Chem., Int. Ed. Engl.*, 2015, vol. 54, p. 14057.
22. Adonin, S.A., Gorokh, I.D., Novikov, A.S., et al., *Chem.-Eur. J.*, 2017, vol. 23, p. 15612.
23. Adonin, S.A., Perekalin, D.S., Gorokh, I.D., et al., *RSC Adv.*, 2016, vol. 6, p. 62011.
24. Usoltsev, A.N., Adonin, S.A., Novikov, A.S., et al., *CrystEngComm*, 2017, vol. 19, p. 5934.
25. Adonin, S.A., Gorokh, I.D., Abramov, P.A., et al., *Eur. J. Inorg. Chem.*, 2017, p. 4925.
26. Adonin, S.A., Gorokh, I.D., Novikov, A.S., et al., *Dalton. Trans.*, 2018, vol. 47, p. 2683.
27. Adonin, S.A., Gorokh, I.D., Novikov, A.S., et al., *CrystEngComm*, 2018, vol. 20, p. 7766.
28. Adonin, S.A., Bondarenko, M.A., Abramov, P.A., et al., *Chem.-Eur. J.*, 2018, vol. 24, p. 10165.
29. Adonin, S.A., Udalova, L.I., Abramov, P.A., et al., *Chem.-Eur. J.*, 2018, vol. 24, p. 14707.
30. Kang, Y.-S., Lu, Y., Chen, K., et al., *Coord. Chem. Rev.*, 2019, vol. 378, p. 262.
31. Arai, T., Horigane, K., Watanabe, O., et al., *iScience*, 2019, vol. 12, p. 280.
32. Cheng, M., Lobkovsky, E.B., and Coates, G.W., *J. Am. Chem. Soc.*, 1998, vol. 120, p. 11018.
33. Nagae, H., Aoki, R., Akutagawa, S., et al., *Angew. Chem., Int. Ed.*, 2018, vol. 57, p. 2492.
34. Zhang, R., Wang, L., Xu, C., et al., *Dalton Trans.*, 2018, vol. 47, p. 7159.
35. Zhou, H.-F., Liu, B., Hou, L., et al., *Chem. Commun.*, 2018, vol. 54, p. 456.
36. Agarwal, R.A., Gupta, A.K., and De, D., *Cryst. Growth Des.*, 2019, vol. 19, p. 2010.
37. Ward, M.D., *Coord. Chem. Rev.*, 2007, vol. 251, p. 1663.
38. Bünzli, J.-C.G. and Eliseeva, S., in *Comprehensive Inorganic Chemistry II*, Reedijk, J. and Poeppelmeier, K, Eds., Amsterdam: Elsevier, 2013, p. 339.
39. Xu, L.-J., Xu, G.-T., and Chen, Z.-N., *Coord. Chem. Rev.*, 2014, vols. 273–274, p. 47.
40. Litvinova, Y.M., Gayfulin, Y.M., Samsonenko, D.G., et al., *Polyhedron*, 2016, vol. 115, p. 174.
41. Mikhalyova, E.A., Yakovenko, A.V., Zeller, M., et al., *Inorg. Chem.*, 2015, vol. 54, p. 3125.
42. Frisenda, R., Janssen, V.A.E.C., Grozema, F.C., et al., *Nat. Chem.*, 2016, vol. 8, p. 1099.
43. Koo, J.Y., Yakiyama, Y., Lee, G.R., et al., *J. Am. Chem. Soc.*, 2016, vol. 138, p. 1776.
44. Sato, O., *Nat. Chem.*, 2016, vol. 8, p. 644.
45. Nikolaevskii, S.A., Evstifeev, I.S., Kiskin, M.A., et al., *Polyhedron*, 2018, vol. 152, p. 61.
46. Fomina, I.G., Chernyshev, V.V., Velikodnyi, Y.A., et al., *Russ. Chem. Bull.*, 2013, vol. 62, p. 427.
47. SMART (control) and SAINT (integration) Software. Version 5.0, Madison: Bruker AXS Inc., 1997.
48. Krause, L., Herbst-Irmer, R., Sheldrick, G.M., and Stalke, D., *J. Appl. Crystallogr.*, 2015, vol. 48, p. 3.
49. Sheldrick, G.M., *Acta Crystallogr., Sect. A: Found. Crystallogr.*, 2008, vol. 64, p. 112.
50. Frisch, M.J., Trucks, G.W., Schlegel, H.B., et al., *Gaussian 09 (Revision E.01)*, Wallingford: Gaussian Inc., 2013.
51. Kohn, W. and Sham, L.J., *Phys. Rev.*, 1965, vol. 140, p. A1133.
52. Starikov, A.G., Minyaev, R.M., and Minkin, V.I., *J. Mol. Struct.: THEOCHEM*, 2009, vol. 895, p. 138.
53. Starikova, A.A., Starikov, A.G., and Minkin, V.I., *Russ. J. Coord. Chem.*, 2015, vol. 41, p. 487. https://doi.org/10.1134/S1070328415080060
54. Nikolaevskii, S.A., Kiskin, M.A., Starikova, A.A., et al., *Russ. Chem. Bull.*, 2016, vol. 65, p. 2812.
55. Nikolaevskii, S.A., Kiskin, M.A., Starikov, A.G., et al., *Russ. J. Coord. Chem.*, 2019, vol. 45, p. 273. https://doi.org/10.1134/S1070328419040067
56. Chemcraft. Version 1.7. 2013. http://www.chemcraft-prog.com.
57. Alvarez, S., Avnir, D., Llunell, M., and Pinsky, M., *New J. Chem.*, 2002, vol. 26, p. 996.
58. Kiskin, M.A., Varaksina, E.A., Taydakov, I.V., and Eremenko, I.L., *Inorg. Chim. Acta*, 2018, vol. 482, p. 85.
59. Flörke U., *CSD Commun.*, 2016 (CCDC 752690 (ZAJNIK)).

Translated by Z. Svitanko